

Equidistant Snakes: Accurate Irregular Shaped Contour Detection

Iván Valdés*
 School of Engineering
 Nagoya University

Yoshihiko Nomura*
 School of Engineering
 Nagoya University

Yasunaga Mitsuya*
 School of Engineering
 Nagoya University

Abstract

Delineation of irregular shaped objects can be realized using active contours, called snakes[1]. However, the minimization of the potential energy pushes the control points toward the lowest potential energy regions, so most of the control points lie in those regions and a few, or even no control points lie in other parts of the contours, as shown in the Fig.1. We propose an Equidistant Snake that forces its control points to be equidistant from each other while minimizing its energy. In this way, it can be assured that the control points will lie all along the contour at equidistant intervals and not only in those regions of higher energy, allowing much more accurate delineation than using standard snakes. We also present a method to create the potential field where the minimum points are on the ridge lines of the edge image, as well as, a method to calculate the weighting factor between the internal energy and the image energy. Finally, we show the behavior of our equidistant snakes in delineating irregular boundaries of some synthesized and medical images.

I The Problem with Irregular Contours

The magnitude of the edge intensity is different in each part of the true edge line, therefore, if we simply minimize the image energy, the control points will concentrate on the

places where the edge intensity becomes a local minimum. So, the control points will be relatively sparse in the places where the edge intensity is low and they will not be uniformly distributed along the ridge line.

The Figure 1 shows an irregular contour and the result after convergence using a standard snakes.

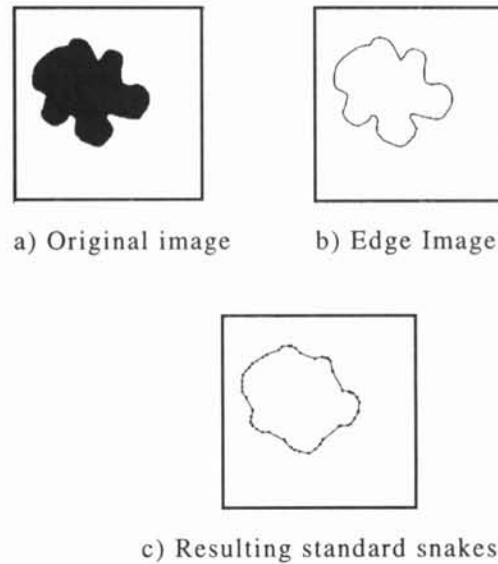


Figure 1: Standard snakes detection

II Equidistant Snakes

2.1 Energy Formulation

The equidistant snakes energy functional to be minimized is defined in the same way as the standard snakes. That is:

*Address: Furo-cho, Chikusa-ku, Nagoya-shi, 464-01, Japan.

e-mail: nomura@mitsuya.nuem.nagoya-u.ac.jp

$$E(U,L)= E_{image}(U) + \lambda E_{int}(L) \quad (1)$$

U is the set of all control points vectors $u_i=[u_i,v_i]^t$, that is,

$$U = \{ u_1, u_2, \dots \}, \quad E_{image} = \sum_{u_i \in U} p(u_i) \quad (2)$$

where $p(u_i)$ is the potential energy at point u_i .

L is the set of all the links joining the control points, so

$$L = \{ l_1, l_2, \dots \} \text{ and } l_m(u_i, u_j)=u_i - u_j, \quad (3)$$

for all i and j joined by a link l_m . So, we define the internal energy as

$$\lambda E_{int}(L)=\frac{1}{2}\lambda \sum_{l_m \in L} \|l_m\|^2 \quad (4)$$

where λ is the regularization parameter[1],[2].

The internal energy causes each control point to move to the position of the gravity center of its connected control points.

2.2 The Potential Image

Using the ordinary Gaussian convolution to calculate the potential image results in the minimum points deviating from the true ridge lines whenever the curvature is large, Fig.2 c).. So, we take the minimum value among the potentials created by the surrounding pixels, Fig.2 d). We will call this resulting image the potential image.

Here, the gradient image is calculated applying the Finite Difference Method (FDM) using the central differences of the intensity gray level image.

Applying the Gaussian convolution, we obtain an expression for the potential p' , at pixel u_j :

$$p'(u_j, w_i) = -g(w_i) e^{-\frac{\|u_j - w_i\|^2}{2\sigma^2}} \quad (5)$$

where $g(w_i)$ is the gradient.

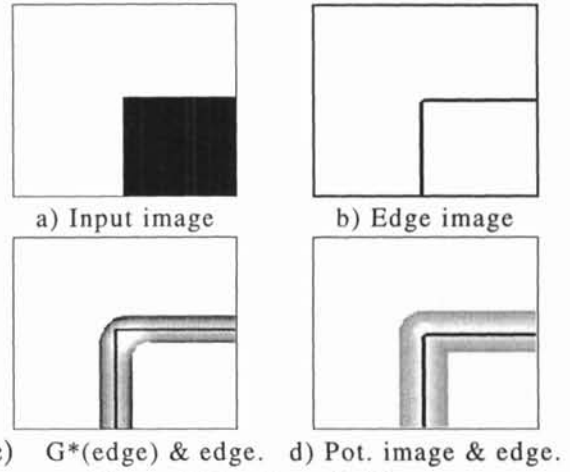


Figure 2: The Potential image.

Finally, the potential image, for each point u_j is:

$$p(u_j) = \min_{w_i} p'(u_j, w_i) \quad (6)$$

2.3 Movement of Control Points

Control points move based on two considerations, the minimization of its energy functional and the equidistant restriction.

Then, each point continues to move until the direction of its former motion vector becomes opposite to that of the actual motion. At this time, the point is considered to have gone through its optimum, i.e., a ridge line, then it stops its motion until all the points have gone through their optimum.

As a step length, we use a factor α that decrements its value in half whenever all the points cross the ridge lines, instead the ordinary steepest descent factor. Thus, the motion vector for each control point, u_i , could be represented

by the following vector:

$$\Delta u_i^{grad} = -\alpha \frac{\left(\frac{\partial E(U, L)}{\partial u_i}\right)'}{\left\|\left(\frac{\partial E(U, L)}{\partial u_i}\right)'\right\|} \quad (7)$$

$$\text{where, } \frac{\partial E(U, L)}{\partial u_i} = \frac{\partial \phi(u_i)}{\partial u_i} + \lambda \sum_{u_j \in U^i} (u_i - u_j) \quad (8)$$

and $U^i = \{u_j \mid \exists I_m(u_i, u_j)\}$

2.4 Equidistant Correction

Our method of achieving equidistance is based on a very simple but important property: *All the control points are equidistant only when they are on the bisector line of its neighboring two control points.*

We modify the motion vector, for each control point, to ensure that they will be on the bisector line. From (7), we calculate the vector Δu_i , the final motion vector, as follows (Figure 3):

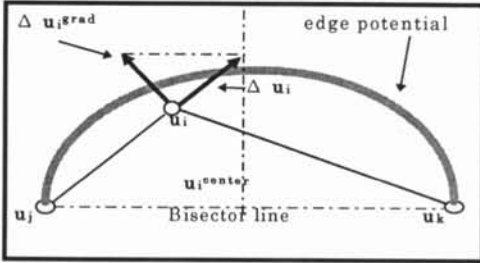


Figure 3: Motion correction vector

$$\Delta u_i = \Delta u_i^{grad} + \frac{(u_k - u_j)'(u_i^{center} - (u_i + \Delta u_i^{grad}))}{\|u_k - u_j\|^2} (u_k - u_j) \quad (9)$$

$$\text{where } u_i^{center} = \frac{u_j + u_k}{2} \quad (10)$$

III Weighting Factor, λ

Let's suppose that, in figure 4, the gradient is

equal to g and the bending angle of the contour equal 2θ . Let's, also, suppose that the control points u_i , u_j and u_k deviate a distance σ from the edge line. In this situation, the condition that u_i no longer deviates from the true contour is given by:

$$\|F_{int}\| \leq \|F_{image}\| \quad (11)$$

And from (5) and (7) we have

$$\|F_{int}\| = 2\lambda d \cos\theta, \quad \|F_{image}\| = \frac{g \sin\theta}{\sigma\sqrt{e}} \quad (12)$$

$$\text{where } \lambda \leq \frac{g \tan\theta}{2d\sigma\sqrt{e}} \quad (13)$$

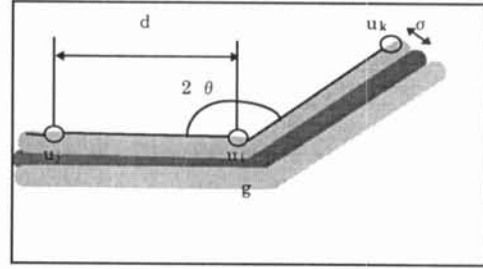


Figure 4: Adjusting of λ

IV Experiments

In our experiments, we defined a measure of the equidistant error for the links as

$$\overline{Error(\%)} = \frac{\sigma_l / \bar{l}}{l} * 100 \quad (14)$$

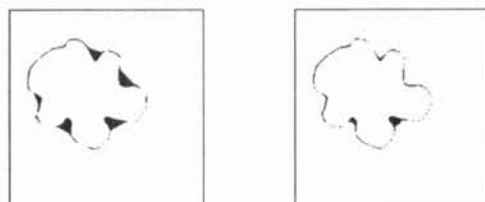
Where \bar{l} is the average of the link lengths, and

σ_l is the standard deviation.

We found that it was about a 60% for the case of standard snakes, compared with a 10% for our equidistant snakes.

We also measured the error in accuracy. Fig.5 shows the residual images for the equidistant and

standard snakes. In the case of equidistant snakes, the error was less than half the error of the standard snakes (given the error as the summation of black areas over the original image area).



a) Standard snakes b) Equid. snakes

Figure 5: Error in accuracy

Fig.6 shows how the accuracy of snakes changes when the number of control points changes for the equidistant and non equidistant snakes.

Fig.7 shows the result of using snakes in a natural image from a cell of blood.

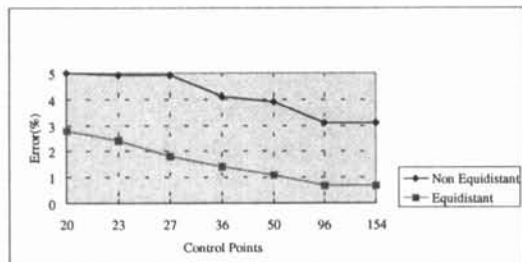
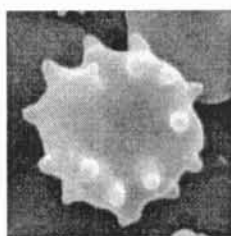
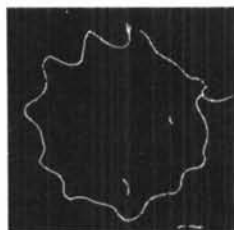


Figure 6: Snakes accuracy comparison.



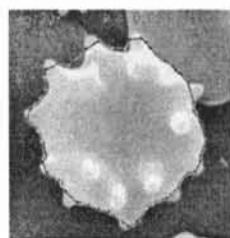
a) Original



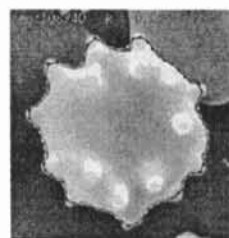
b) Edge image



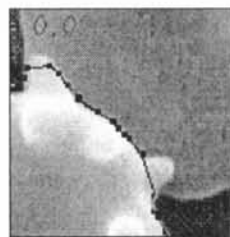
c) Pot. image



d) Standard snakes



e) Equid. snakes



f) Std. snakes (Zoom)



g) Equid. snakes (Zoom)

Figure 7: Equidistant and standard snakes performance in a natural image.

V Conclusion

We have introduced an equidistant snake that adjusts its control points in order to delineate irregular shaped contours more accurately. This equidistant snake has proven to be especially useful for applications such as segmenting and tracking of medical images. We have also presented a method to create a potential field, as well as, a design method to calculate the regularization factor λ .

References

- [1] M. Kass, A. Witkin, and D. Terzopoulos, "Snakes: Active Contour Models.", Proc. 1st. Int. Conf. on Comp. Vision, 1987, pp. 259-269.
- [2] K. F. Lai, and R. T. Chin, "On Regularization, Formulation and Initialization of the Active Contour Models (Snakes).", Proc. Asian Conf. on Comp. Vision, 1993, pp. 542-545.